Development/Plasticity/Repair

Control of Precerebellar Neuron Development by *Olig3* bHLH Transcription Factor

Zijing Liu,[1] Hong Li,[1] Xuemei Hu,[1] Ling Yu,[2] Hongbin Liu,[2] Ruifa Han,[3] Rita Colella,[1] George D. Mower,[1] Yiping Chen,[2] and Mengsheng Qiu[1,3]

[1]Department of Anatomical Sciences and Neurobiology, University of Louisville School of Medicine, Louisville, Kentucky 40202, [2]Department of Cell and Molecular Biology, Tulane University, New Orleans, Louisiana 70117, and [3]Institute of Urological Surgery, Tianjin Medical University, Tianjin 300211, China

The rhombic lip (RL) is the neuroepithelium immediately adjacent to the roof plate of the fourth ventricle, and it gives rise to various brainstem and cerebellar cell types. Our study shows that the bHLH (basic helix-loop-helix) transcription factor *Olig3* is expressed in the progenitors of RL, and ablation of *Olig3* significantly affects the development of RL. In *Olig3*−/− caudal RL, the expression level of *Math1* in the dorsal interneuron 1 (dI1) domain is reduced, and the formation of four mossy-fiber nuclei is compromised; dI2–dI3 neurons are misspecified to dI4 interneurons, and the climbing-fiber neurons (inferior olive nucleus) are completely lost. In addition, the formation of brainstem (nor)adrenergic centers and first-order relay visceral sensory neurons is also dependent on *Olig3*. Therefore, *Olig3* plays an important role in the fate specification and differentiation of caudal RL-derived neurons.

Key words: **bHLH; cell fate; rhombic lip; mossy-fiber nuclei; climbing-fiber nucleus; cerebellum**

Introduction

The rhombic lip (RL) is a specific germinal matrix that is located in the dorsal hindbrain neuroepithelium between the roof plate of fourth ventricle and neural tube. Along the anterior–posterior axis of the rhombomeres, the RL is divided into rostral and caudal parts (Lumsden and Krumlauf, 1996). The rostral RL (rRL) is related to the neuroepithelium of rhombomere 1 (r1) and specifically expresses basic helix-loop-helix (bHLH) transcription factor *Math1*. The neurons derived from rRL migrate along the rostral rhombic-lip migratory stream and sequentially populate a series of nuclei within the rostral hindbrain and cerebellum, of which most are *Math1* dependent (Machold and Fishell, 2005; Wang et al., 2005). In cerebellum, rRL gives rise to glutamatergic external granule layer (EGL) cells, large deep cerebellar nuclei (DCN) neurons, and unipolar brush cells.

The caudal RL (cRL) (r2–r5) comprises the auditory lip and gives rise to the cochlear extramural migratory stream (EMS) to form the cochlear nuclei (CN) (Farago et al., 2006). The generation of ventral CN and cochlear granule neurons requires *Math1* expression (Wang et al., 2005). The more caudal cRL (r6–r8) produce the precerebellar mossy-fiber (MF) nuclei and climbing-fiber (CF) nuclei (Ambrosiani et al., 1996; Cambronero and Puelles, 2000). There are four major MF nuclei that project mossy fibers to the EGL and DCN, including the pontine gray nuclei (PGN), reticulotegmental nuclei (RTN), lateral reticular nuclei (LRN), and external cuneate nuclei (ECN). The PGN and RTN migrate in the anterior precerebellar EMS (AES) and settle in the rostral-ventral region of the pons, whereas the LRN and ECN migrate in the posterior precerebellar EMS (PES) and settle in the medial-dorsal and lateral-ventral region of medulla, respectively (Altman and Bayer, 1987a,b,c,d). Loss of *Math1* completely inhibits the formation of AES and PES and the generation of four MF nuclei (Wang et al., 2005). In contrast, the inferior olive nucleus (ION) projects climbing fibers to the Purkinje cells, forming the olivocerebellar circuit (Altman and Bayer, 1987a,b,c,d; Sotelo, 2004). The ION migrates from the cRL via the precerebellar intramural migratory stream (IMS) and settles in the medial-ventral region of the medulla (Altman and Bayer, 1987a,b,c,d). The generation of ION is *Math1* independent, but the migration of CF neurons requires *Ptf1a*, which is expressed ventral to the *Math1* domain (Yamada et al., 2007).

Previous studies showed that *Olig3* bHLH transcription factor was expressed in the RL (Takebayashi et al., 2002). In this study, we showed that *Olig3* was specifically expressed in dorsal progenitor 1 (dp1)–dp3 domains of neural progenitor cells in the caudal hindbrain (r6–r8) and regulated the fates of these neural progenitor cells. In *Olig3* mutant hindbrain, the cell fate of dp2 and dp3 progenitors was changed to that of the more ventral interneuron progenitors. The generation of four MF nuclei was markedly reduced. More strikingly, ION CF neurons were completely lost, providing evidence that these neurons may arise from the ventral dorsal interneuron 3 (dI3) domain, which is dependent on both *Olig3* and *Ptf1a*. In addition, development of dorsal *Phox2b*+ neurons, brainstem (nor)adrenergic centers, and first-order relay visceral sensory neurons was also disrupted.

Received Aug. 10, 2008; accepted Aug. 30, 2008.

This work was supported by the National Institutes of Health Grants R21 NS 060033, R01 NS37717, and R01EY016724. We thank Drs. Hirohide Takebayashi, Carmen Birchmeirer, Helena Edlund, and Jane Johnson for generously providing the anti-Olig3, anti-Lbx1, anti-Tlx3, anti-Ngn1, and anti-Ptf1a antibodies.

Correspondence should be addressed to Mengsheng Qiu at the above addresses. E-mail: m0qiu001@louisville.edu.

DOI:10.1523/JNEUROSCI.3769-08.2008

 0270-6474/08/2810124-10$15.00/0

Materials and Methods

Generation of Olig3 *knock-out mice.* A BAC clone containing *Olig3* genomic DNA was purchased from Invitrogen. The *Olig3* targeting vector contained a 4 kb 5′ arm and a 3.5 kb 3′ arm at the two ends of *neo* cassette. Targeting vector was linearized and electroporated into mouse embryonic stem (ES) cells. G418-resistant cells were selected. Genomic DNA from drug-resistant cells was digested with enzyme and analyzed by Southern hybridization using 5′ or 3′ probe for *Olig3*. Chimeric mice and F1 heterozygous mice were generated from *Olig3* mutant ES cell lines. Germline transmission of the target allele was confirmed by both Southern analysis and PCR.

In situ *RNA hybridization and immunofluorescent staining.* Brain tissues were isolated from embryonic day 10.5 (E10.5)–E18.5 mouse embryos and then fixed in 4% paraformaldehyde at 4°C overnight. After fixation, tissues were transferred to 20% sucrose in PBS overnight, embedded in OCT media, and then sectioned (20 μm thickness) on a cryostat. Sections at similar positions from the wild-type and mutant embryos were subsequently subjected to *in situ* hybridization (ISH) or immunofluorescent staining. ISH was performed as described by Schaeren-Wiemers and Gerfin-Moser (1993) with minor modifications. cDNA templates for ISH were obtained either by reverse transcription-PCR of postnatal day 0 brain tissues or from a commercial source (Invitrogen), and confirmed by sequencing.

Immunofluorescent staining was performed as follows. After rinsing with PBS, sections were permeabilized in 0.1% Triton X-100 in PBS for 10 min, rinsed with PBS to remove the excessive Triton, incubated in blocking solution (5% normal serum in PBS plus 1% BSA) at room temperature for 1 h, and incubated in diluted primary antibody in blocking solution at 4°C overnight. On the next day, sections were washed in PBS three times for 10 min each, and incubated with the secondary antibody in blocking solution at room temperature for 1 h. After incubation, sections were washed in PBS three times for 10 min each, before they were mounted in Mowiol mounting medium on glass slides. The staining was examined under a Nikon fluorescence microscope. Rat polyclonal antibody anti-Olig3 was generously provided by Dr. Hirohide Takebayashi. Rabbit polyclonal antibody anti-Ngn1 was kindly provided by Dr. Qiufu Ma. Guinea-pig polyclonal antibody anti-Ptf1a was kindly provided by Dr. Jane Johnson. Rabbit polyclonal antibody anti-Ptf1a was kindly provided by Dr. Helena Edlund. Anti-Brn3a (1:200; Millipore Bioscience Research Reagents), anti-Mash1 (1:400; BD Biosciences), and anti-Pax2 (1:200; Zymed) were obtained from commercial sources. Guinea-pig polyclonal antibody anti-Lbx1 and rabbit polyclonal antibody anti-Tlx3 were kindly provided by Dr. Carmen Birchmeier. The Alexa-488- or Alexa-594-conjugated secondary antibodies were obtained from Invitrogen. The nucleic acid dye DAPI (4′,6-diamidine-2′-phenylindole dihydrochloride) was obtained from Roche.

Olivocerebellar projection tracing with DiI. Brain tissues were isolated from E18.5 mouse embryos and fixed in 4% paraformaldehyde. Single or multiple small crystals of DiI were placed in one side of the cerebellar hemisphere far from the midline in E18.5 wild-type or *Olig3*−/− animals. Tissues were stored in 4% paraformaldehyde in dark at 37°C. After 5–6 weeks for DiI diffusion, tissues were transferred to 20% sucrose in PBS overnight, embedded in OCT media, and then sectioned (30 μm thickness) on a cryostat. The DiI staining was examined under a Nikon fluorescence microscope.

Results

Olig3 expression pattern in the rhombic lip

It has been well documented that several nuclei in the hindbrain originate from the rhombic lip. A previous report and our present studies demonstrated that *Olig3* is expressed in the rhombic lip in the entire hindbrain, isthmus area, and the subventricular zone of cerebellum and pons (Fig. 1*A*,*B*) (Takebayashi et al., 2002). To investigate the function of *Olig3* in the development of hindbrain, we performed detailed studies on the expression pattern of *Olig3* in cRL at early embryonic stages by comparing *Olig3* expression with various specific interneuron markers. Similar to that in the dorsal spinal cord, the dorsal neuroepithelium in the caudal hindbrain could be divided into several domains along the dorsal–ventral axis based on the expression of multiple interneuron markers (Sieber et al., 2007). At early stages of neural development, *Math1* and *Ngn1* specifically label the progenitor pool of dp1 and dp2, respectively, whereas *Tlx3* marks dI3 and dI5 interneurons (Gowan et al., 2001; Qian et al., 2002; Sieber et al., 2007). Because the dorsal *Ngn1* expression was only detected in cRL at r7–r8 level, which lies between the otic vesicle and cervical spinal cord (Landsberg et al., 2005), we used *Ngn1* as the rostral–caudal boundary marker. At E10.5, *Olig3* marked the dorsalmost domains (dp1–dp3) of neuroepithelium in the caudal hindbrain and was colabeled with *Math1*, *Ngn1*, and *Tlx3*, respectively (Fig. 1*C–E*,*G*,*H*). There was no *Olig3* expression detected in dp4–dp6 domains, from which *Pax2*-labeled dI4 and dI6 neurons arose (Fig. 1*I*) (Helms and Johnson, 2003; Mizuguchi et al., 2006). There was a partially overlapping region between *Olig3* and *Ptf1a* in the ventral dp3 domain (Fig. 1*C*,*F*,*K*). The overlapping expression of *Olig3* and *Ptf1a* in the dorsal neuroepithelium became more apparent at E11.5 (Fig. 2*A*). This overlapping domain appeared to be tightly associated with the generation of Brn3a+ glutamatergic neurons, instead of the Pax2+ GABAergic inhibitory neurons (Fig. 2*B*,*C*), in keeping with the recent observation that Brn3a+ CF neurons were labeled by the Ptf1a-Cre fate mapping experiments (Yamada et al., 2007). *Olig3* remained to be expressed in the dorsal neural progenitor cells at E12.5, but its expression domain was dorsally retracted (Fig. 2*D–F*). Together, these studies indicated that *Olig3* is selectively expressed in the progenitor pool of the cRL at early stages of neurogenesis, suggesting that *Olig3* may be involved in the fate specification and/or migration of the neurons originated from the cRL.

Generation of *Olig3* mutant mice

To elucidate the function of *Olig3* in hindbrain development, we performed gene targeting of *Olig3* by homologous recombination in ES cells. The targeting vector was designed to replace the entire coding region with the neomycin (neo) gene (Fig. 3*A*). After electroporation and drug selection, the ES clones harboring homologous recombination were identified by genomic Southern blot with the flanking probes (Fig. 3*C*). These ES cells were injected into blastocysts, and the targeted alleles were transmitted through germ line. Heterozygous mice were born and mated to obtain homozygous mutant mice. As expected, *Olig3* expression was not detected in the *Olig3*−/− mutants (data not shown). Most *Olig3* homozygous mutants died soon after birth, and few could stay alive until 12 h. *Olig3*−/− mice displayed cyanosis caused by respiratory failure, resembling the congenital hypoventilation syndrome in humans, suggesting that there is a defect in the developing respiratory system, which resides in the brainstem (Shirasawa et al., 2000).

Olig3 regulates the formation of precerebellar mossy-fiber nuclei

To test the possibility that loss of *Olig3* function may affect the development of RL-derived neurons, we first examined the effects of *Olig3* mutation on the correct establishment of brainstem precerebellar nuclei (PCN). There are five major PCN that arise from rhombomere 6–8 cRL. The ION provides climbing fibers to the cerebellum. The remaining four are the MF precerebellar nuclei (PGN, RTN, LRN, and ECN), tangentially migrating from the cRL in the precerebellar EMS. Transcription factor *Barhl1* has been used as a generic marker for migrating and mature MF neurons (Bulfone et al., 2000). Expression analyses on E14.5 hindbrain coronal sections revealed that the expression level of

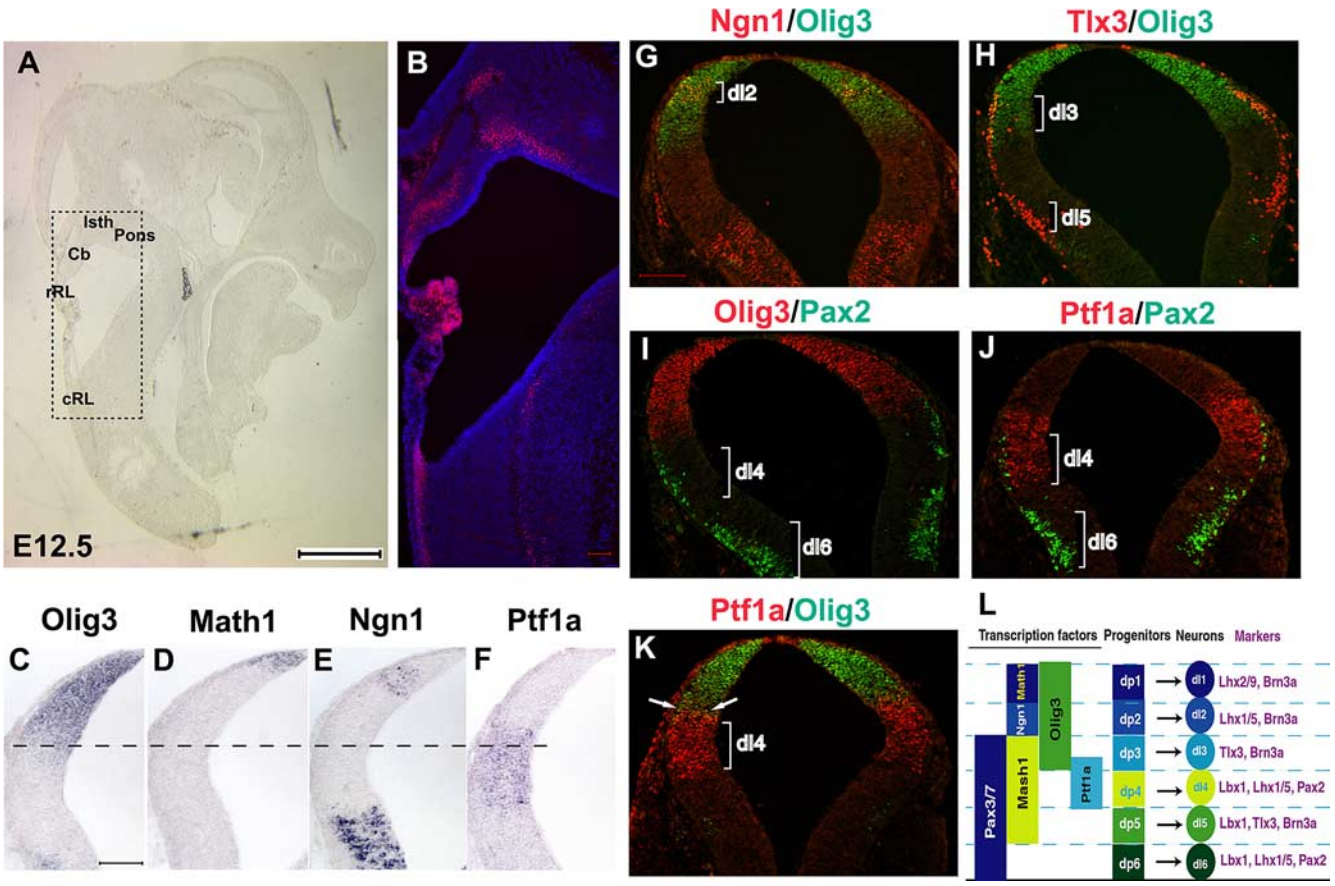

Figure 1. Expression of *Olig3* in the mouse hindbrain. ***A***, Unstained bright-field photograph of E12.5 mouse brain sagittal section. ***B***, *Olig3* expression in E12.5 sagittal hindbrain corresponding to the box position shown in ***A***. ***C–F***, *In situ* hybridization of various progenitor TFs in the dorsal hindbrain at E10.5. All transverse sections are oriented with lateral to the left. *Olig3* expression region included the expression domain of *Math1* (***D***) and *Ngn1* (***E***). There is partial overlap between *Olig3* (***C***) and *Ptf1a* (***F***) expression in dp3 domain. ***G–K***, Double-immunofluorescence analysis of Olig3 expression pattern in E10.5 transverse hindbrain sections at r6 –r8 level. Olig3 expression overlapped with Ngn1 (***G***) and Tlx3 (***H***), but not with Pax2 (***I***) in the dorsal hindbrain. Ptf1a was expressed in dp4 and part of dp3 domains (***J***). Olig3 and Ptf1a were coexpressed in some ventral dp3 progenitors (***K***, arrows). ***L***, Summary of distinct dp domains and dIs in which the transcription factors were expressed. Cb, Cerebellum; Isth, isthmus. Scale bars: ***A***, 1 mm; ***B***, ***C*** (for ***C–F***), ***G*** (for ***G–K***), 100 μm.

Barh1 in EMS was significantly downregulated in *Olig3*−/− mutants compared with wild-type tissues (Fig. 4*A*,*B*). As a result, the formation of four MF nuclei was markedly inhibited in *Olig3*−/− hindbrains, as revealed by *Barhl1* expression in four discrete MF nuclei in E16.5 and E18.5 tissues (Fig. 4*E*,*F*,*I*,*J*,*M*,*N*). Our results showed that transcription factor *Zic1* is also expressed in MF neurons. Compared with wild-type littermates, *Olig3*−/− embryos showed apparently reduced *Zic1* mRNA expression within the area of the EMS and all four MF nuclei, similar to *Barhl1* expression (Fig. 4*A–P*). Together, these findings demonstrated that *Olig3* expression was required for the proper formation of both the EMS and the precerebellar MF nuclei.

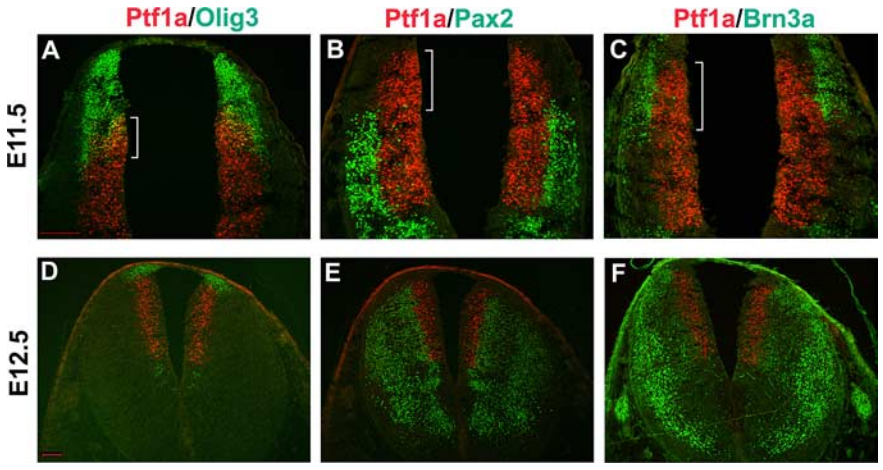

Figure 2. Expression of neural progenitor genes and neuron-specific markers in the dorsal caudal hindbrain. Transverse sections from E11.5 (***A–C***) and E12.5 (***D–F***) rhombomere 7 were subject to double immunostaining with various progenitor and subtype-specific markers. At E11.5, there was a considerable overlapping between *Olig3* and *Ptf1a* (indicated by bracket; ***A***), and this overlapping region was associated with the generation of Brn3a+ excitatory neurons (indicated by bracket; ***C***), but not Pax2+ inhibitory neurons (indicated by bracket; ***B***). Scale bars: ***A*** (for ***A–C***), ***D*** (for ***D–F***), 100 μm.

Olig3 regulates the formation of the inferior olive nucleus

ION is the precerebellar CF nucleus, emigrating from the cRL via the IMS and settling in the most ventral region of caudal medulla (Altman and Bayer, 1987a,b,c,d). The migrating and mature CF neurons can be detected by the expression of Brn3a (Fedtsova and Turner, 1995; Xiang et al., 1996). At E14.5, the Brn3a+ CF neurons in ION were detected at the medulla in the wild-type tissues (Fig. 5*A*), but not in *Olig3*−/− mutants (Fig. 5*B*). The loss of CF neurons in *Olig3*-deficient mutants was further confirmed

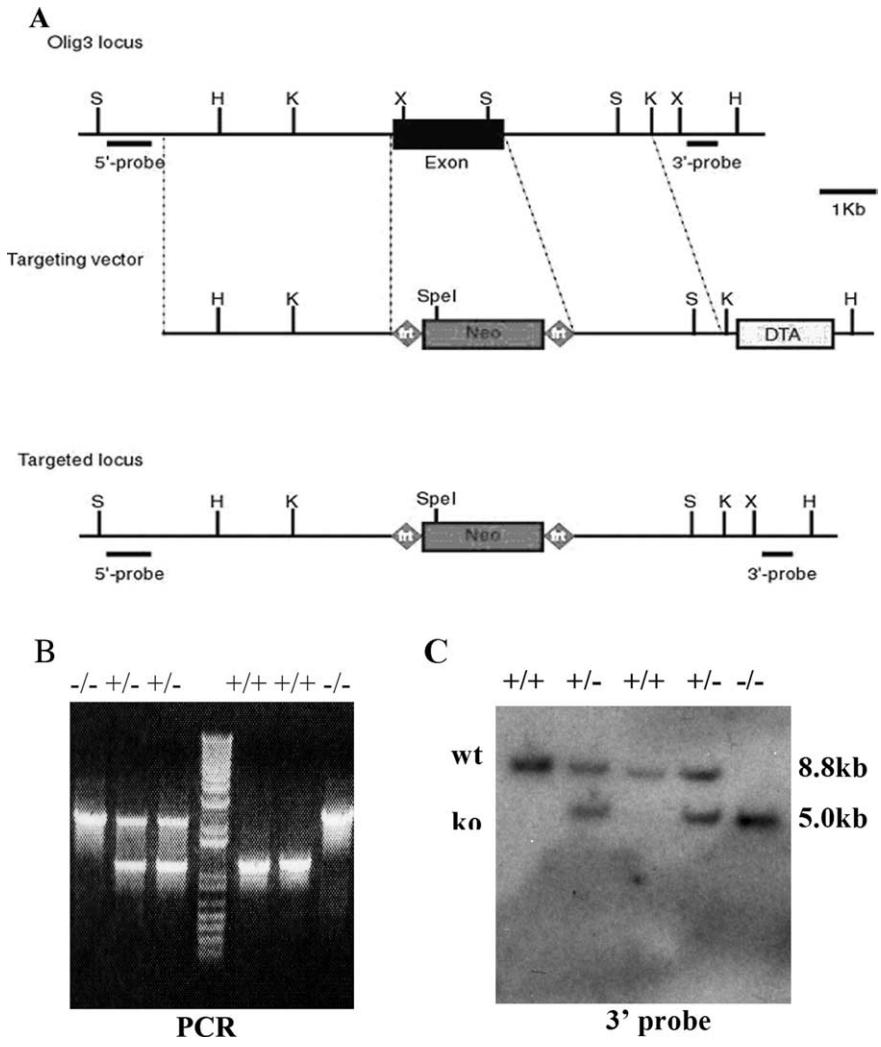

Figure 3. Inactivation of *Olig3* by homologous recombination. ***A***, Schematic of the strategy for *Olig3* gene targeting. The wild-type *Olig3* locus, targeting vector, and the targeted allele after homologous recombination are shown. 5′ and 3′ probes are used for Southern blot analysis. *Neo*, Neomycin positive selection marker cassette; DTA, diphtheria toxin gene negative selection marker. ***B***, PCR analysis of genomic DNA extracted from wild-type, *Olig3*+/−, or *Olig3*−/− tails. ***C***, Genotyping by Southern blot analyses. Genomic DNA was digested with *Hin*dIII and *Spe*I and hybridized with the 3′ probe. The wild-type allele (wt) appeared as a 8.8 kb band and the mutant allele (ko) as a 5.0 kb band.

by the lack of expression of *Rph3a* (Fig. 5*C*,*D*) and *Fgfr2* (data not shown), two other markers for ION neurons (Belluardo et al., 1997; Foletti and Scheller, 2001). The absence of Brn3a and *Rph3a* expression in *Olig3*−/− medulla persisted at E16.5 (Fig. 5*E–H*) and E18.5 (data not shown), indicating that the ION defect was not simply a developmental delay. The loss of ION structure was further confirmed by the lack of Nissl staining in the ION region of the *Olig3* mutants (supplemental Fig. S1, available at www.jneurosci.org as supplemental material).

Because no ectopic Brn3a+ CF neurons were found in *Olig3*−/− medulla, we proposed that ION neurons fail to form possibly as a result of the loss of CF progenitor pool, instead of their incorrect migration route. To examine whether an ectopic olivocerebellar projection existed in *Olig3* homozygote mutants, we performed retrograde labeling of axon fibers in the medulla by placing DiI crystals into one side of E18.5 cerebellum and culturing them for 5 weeks in the dark at 37°C. In the wild-type brains, Purkinje cells incubated with DiI always received the climbing fibers from the contralateral ION (Fig. 5*I*,*K*). However, no DiI labeling of climbing fibers and cell bodies was observed in *Olig3* mutant brain (Fig. 5*J*,*L*), consistent with the idea of the loss of the olivocerebellar circuit. The DiI labeling of the mossy fiber nucleus LRN was detected in the wild-type embryos, but was almost completely lost in *Olig3*−/− medulla (Fig. 5*I–L*), in keeping with the dramatic reduction of expression of LRN marker Zic1 (Fig. 4*G*,*H*). Based on these results, we concluded that *Olig3* expression was indispensable for the generation of CF neurons and LRN mossy fiber neurons.

Olig3 regulates cell fate specification of dp1–dp3

Previous studies showed that the formation of MF nuclei was dependent on *Math1*, but the migration of CF neurons was regulated by *Ptf1a* in cRL (Wang et al., 2005; Yamada et al., 2007). Because *Olig3* is expressed in the *Math1*+, *Ngn1*+, and dorsal part of *Ptf1a*+ domains in cRL, it is possible that *Olig3* may control the formation of MF nuclei and CF nucleus by regulating the expression of *Math1*, *Ngn1*, and *Ptf1a* in the dorsal neural progenitor cells. Consistent with this idea, our expression studies in E10.5 hindbrains revealed a modest reduction of *Math1* (we counted 42 ± 4 and 28 ± 6 *Math1*+ progenitors in control and *Olig3*−/−, respectively) and *Barhl1* expression in dp1 domain (Fig. 6*A–D*), and a nearly complete loss of dorsal *Ngn1* expression in the dp2 domain, although the ventral *Ngn1* expression was not affected (Figs. 6*E*,*F*, 7*E*,*F*). The expression of *Lmx1a* resides immediately dorsal to *Math1* and marks the roof plate. *Lmx1a* expression was similar in control and *Olig3*−/− embryos (Fig. 6*K*,*L*). Interestingly, the expression pattern of *Neo* in *Olig3*−/− mutants was nearly identical to that of the endogenous *Olig3* gene in the wild-type embryos (Fig. 6*G*,*H*), indicating that *Olig3* mutation did not affect the initial allocation and survival of neural progenitors in RL.

Remarkably, *Ptf1a* was upregulated and expanded dorsally into the dorsal dp3 and dp2 domains in *Olig3*-null hindbrain (Fig. 6*I*,*J*). Ectopic expression of Pax2 (dI4 and dI6 marker) and Lbx1 (dI4–dI6 marker) was also detected at the positions of dI2 and dI3 interneurons (Fig. 7*A–D*). The dorsal expansion of Ptf1a and Pax2 expression was accompanied by the reduced expression of Brn3a in dI1–dI3 dorsal interneurons and the absence of Brn3a+ IMS in the *Olig3*−/− hindbrain (Fig. 7*A*,*B*; supplemental Fig. S2, available at www.jneurosci.org as supplemental material). In contrast, Brn3a+ dI5 interneurons persisted in the mutant embryos. In addition, *Olig3* mutation resulted in the loss of Tlx3+ dI3 interneurons, but not Tlx3+ dI5 neurons (Fig. 7*G*,*H*). Expression of Mash1 (dp3–dp5 marker) was not affected by loss of *Olig3* (Fig. 7*I*,*J*). Together, these observations indicated that in the absence of *Olig3* expression, Brn3a+ dI2 and dI3 neurons were respecified to Pax2+ dI4 neurons. In other words, whereas the Ptf1a+ domain gives rise to both Brn3a+ and Pax2+ neu-

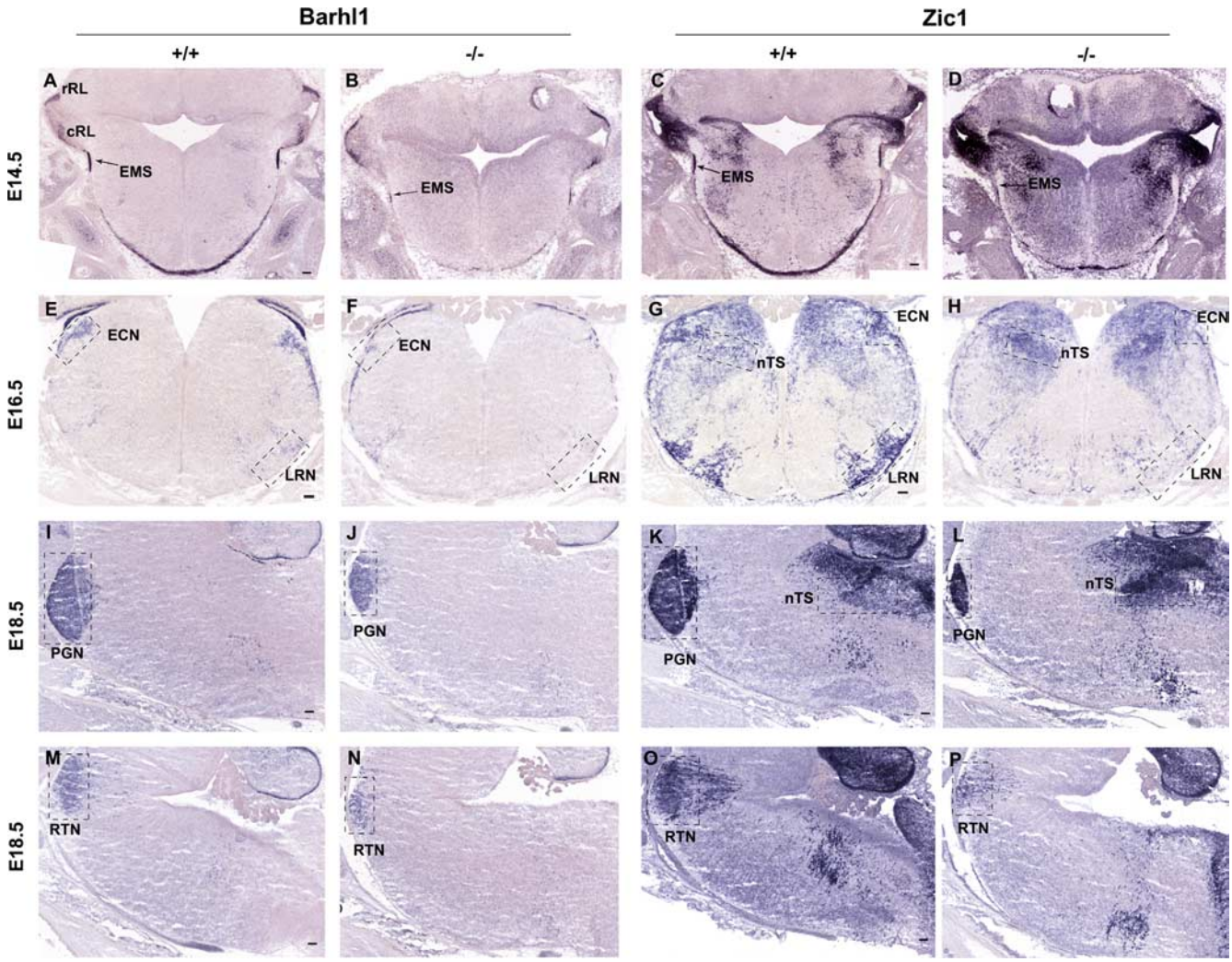

Figure 4. *Olig3* mutation affected the generation of precerebellar mossy-fiber nuclei. ***A–H***, Coronal sections from E14.5 and E16.5 hindbrain tissues were examined by *in situ* hybridization for expression of *Barhl1* (***A***, ***B***, ***E***, ***F***) and *Zic1* (***C***, ***D***, ***G***, ***H***). Both of these genes were expressed in the migrating and mature mossy-fiber neurons. Loss of *Olig3* function significantly downregulated the expression level of these two genes in the EMS and reduced the size of the mature mossy-fiber nuclei, LRN and ECN. ***I–P***, E18.5 sagittal sections with rostral to the left. ***I***, ***J***, ***M***, ***N***, Sections were labeled with *Barhl1* probe. ***K***, ***L***, ***O***, ***P***, Sections were stained with *Zic1* probe. *Olig3*-null embryos displayed the reduced size of two other mossy-fiber nuclei, PGN and RTN. Ectopic *Zic1* expression was detected in the nTS area (***G***, ***H***, ***K***, ***L***). Scale bars: ***A*** (for ***A***, ***B***), ***C*** (for ***C***, ***D***), ***E*** (for ***E***, ***F***), ***G*** (for ***G***, ***H***), ***I*** (for ***I***, ***J***), ***K*** (for ***K***, ***L***), ***M*** (for ***M***, ***N***), ***O*** (for ***O***, ***P***), 100 μm.

rons in wild-type mice, the expanded Ptf1a+ domain in *Olig3*−/− mice only produces Pax2+ neurons.

Olig3 is required for proper formation of the brainstem (nor)adrenergic centers and visceral sensory neurons

Both relay visceral sensory and (nor)adrenergic neurons in the brainstem play crucial roles in regulating respiration pattern and cardiovascular activities, and these two classes of neurons originate from dp3 domain (Qian et al., 2001, 2002). Our studies show that *Olig3*−/− mice die from respiratory failure, suggesting that *Olig3* may affect the generation of these two types of neurons. Because *Phox2b* is essential for formation of brainstem (nor)adrenergic centers and proper development of many visceral sensory neurons (Morin et al., 1997; Pattyn et al., 1999, 2000), we performed a detail examination of *Phox2b* expression in *Olig3*-deficient hindbrains. Dorsal *Phox2b* expression was completely inhibited in E11.5 and E12.5 *Olig3*−/− mutants, whereas its ventral expression in the dorsal motor nucleus of vagus (dmnX) was normal (Fig. 8*A–D*). At later stages, *Phox2b* expression was completely eliminated in the prospective nucleus of the solitary tract (nTS) area in the *Olig3*−/− hindbrain (Fig. 8*E*,*F*,*I*,*J*). The first-order relay visceral sensory neurons in the nTS receive signals generated from peripheral chemoreceptors and pulmonary stretch receptors and then influence respiration rates (Blessing, 1997). In addition, the expression level of *Phox2b* was reduced in the pons as well (Fig. 8*I*,*J*). In contrast, *Phox2b* expression in other brainstem structures was not affected, including the dmnX and nucleus ambiguus (Fig. 8*E*,*F*,*I*,*J*). Instead, ectopic *Zic1* expression was detected at the nTS area in E16.5 and E18.5 *Olig3*−/− medulla (Figs. 4*G*,*H*, 8*G*,*H*). To determine the stages when ectopic migration of *Zic1*+ neurons occurs, we examined *Zic1* expression in *Olig3* mutant embryos at earlier stages. At E10.5, *Zic1* expression was normal in the ventricular zone throughout the entire dorsal hindbrain (data not shown). At E12.5, *Zic1*+ neurons derived from dp1 and dp4 domains formed two ventrally migratory streams in wild-type embryos, whereas *Zic1*+ neurons from the entire dp1–dp4 region were able to migrate ventrally in *Olig3*−/− hindbrains (supplemental Fig. S3*A–D*, available at www.jneurosci.org as supplemental material), further supporting the notion that dI2–dI3 neurons are misspecified to dI4 interneurons and behave like dI4 neurons. However, misspecified dorsal interneurons still took their migra-

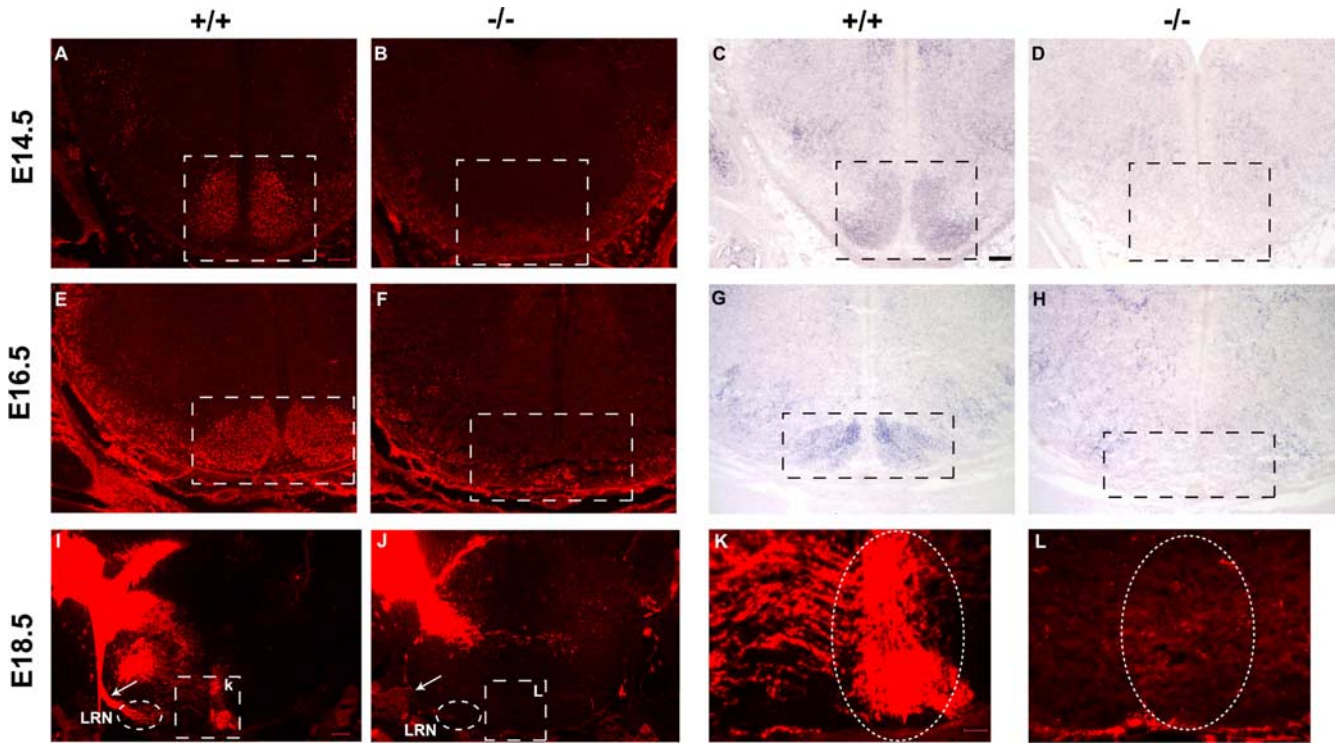

Figure 5. The *Olig3*−/− mutant lost the precerebellar climbing-fiber neurons. ***A–H***, E14.5 (***A–D***) and E16.5 (***E–H***) coronal medulla sections were subjected to immunostaining with anti-Brn3a antibody (***A***, ***B***, ***E***, ***F***) or *in situ* hybridization with *Rph3a* probe (***C***, ***D***, ***G***, ***H***). Both genes were expressed in the climbing-fiber neurons. ION comprised of climbing-fiber neurons was lost in *Olig3*-null medulla. ***I–L***, DiI labeling was used to examine the formation of the olivocerebellar projection in E18.5 tissues. DiI crystal was placed into one side of wild-type cerebellum, and projections (arrow) to the contralateral ION (circled area) were detected (***I***, ***K***). However, the formation of the DiI labeling olivocerebellar projection was not detected in the *Olig3*−/− mutant (***J***, ***L***). In addition, DiI labeling of LRN neurons was drastically reduced as well in the mutant (small circled area; ***I***, ***J***). The dashed boxes in ***A–J*** outline the ION area. ***K***, ***L***, High-magnification images of ***I*** and ***J***. Scale bars: ***A*** (for ***A***, ***B***, ***E***, ***F***), ***C*** (for ***C***, ***D***, ***G***, ***H***), 100 μm; ***I*** (for ***I***, ***J***), 200 μm; ***K*** (for ***K***, ***L***), 50 μm.

tion path to the nTS area, which is normally occupied by *Phox2b*+ neurons derived from dI3 domain (Fig. 8*G*,*H*) (Qian et al., 2001). Consistent with this idea, ectopic expression of *Viaat*, GABAergic neuron marker, was detected at the nTS area in E18.5 *Olig3*-deficient embryos (supplemental Fig. S3*E–H*). This finding is in keeping with the observations that *Ptf1a* promoted neural precursors to differentiate into GABAergic neurons (Hoshino et al., 2005; Mizuguchi et al., 2006) and was ectopically expressed in dp2 and dp3 domains in *Olig3*−/− hindbrain (Fig. 6*I*,*J*).

Our results also showed that loss of *Olig3* function affected the formation of (nor)adrenergic centers. The generation of the A1/C1 and A2/C2 clusters in the medulla was completely absent in *Olig3*−/− brainstems, as indicated by the lack of expression of tyrosine hydroxylase (TH) (Fig. 8*K*,*L*). In summary, loss of *Olig3* function completely inhibited the generation of *Phox2b*+ neurons derived from the cRL dp3 domain and disrupted the formation of brainstem (nor)adrenergic centers and first-order relay visceral sensory neurons.

Discussion

In this study, we present evidence that *Olig3* is primarily expressed in RL cells in the developing hindbrain and that its expression is important for the fate specification of RL progenitor cells. In the absence of *Olig3* function, development of precerebellar neurons derived from the caudal RL is either reduced or completely inhibited. Additionally, *Olig3* plays a critical role in regulating the formation of the central respiratory system.

Olig3 is predominantly expressed in RL cells in the hindbrain

The RL was first reported as the germinal zone immediately adjacent to the roof plate of the fourth ventricle through morphological studies (His, 1891). The diversity of neurons in the mature brain is proposed to be generated from this neuroepithelium and to migrate to their destination. Although many attempts have been made, the exact distinction between the RL and the adjacent neuroepithelium still remains unclear. Our studies suggest that *Olig3* can be used as a candidate molecular marker for labeling RL cells based on the following observations. (1) *Olig3* is expressed in the RL throughout the anterior–posterior axis of the rhombomere (Fig. 1*B*) (Takebayashi et al., 2002). (2) No *Olig3* expression is detected in the roof plate, and the mutation of *Olig3* is not related to the development of the roof plate (Fig. 6*G*,*K*,*L*). (3) *Olig3* is expressed in the *Math1*+ and dorsal part of *Ptf1a*+ domains in cRL, from which MF neurons and CF neurons arise (Fig. 1). (4) *Olig3* mutation reduces the generation of MF nuclei and completely inhibits the formation of CF nucleus. Together, these observations strongly suggest that *Olig3* predominantly labels RL progenitor cells in the entire hindbrain.

Origin and molecular specification of ION neurons in the caudal hindbrain

Our data showed that *Olig3* is specifically expressed in dp1–dp3 domains of the caudal hindbrain at r6–r8 level (Fig. 1*C–K*). It is well known that *Math1* is specifically expressed in the dp1 domain and determines the cell fate of dI1 neurons that substantially form the precerebellar MF neurons (Wang et al., 2005). Loss of *Olig3* leads to a modest downregulation of *Math1* expression (Fig. 6*A*,*B*) and partial reduction of four MF nuclei in the brainstem (Fig. 4). Although the origin of the MF neurons has been well defined, it remains unclear from which region of cRL the precerebellar CF neurons are derived. Classical ablation experiments indicated that removal of the dorsal third of the neuroep-

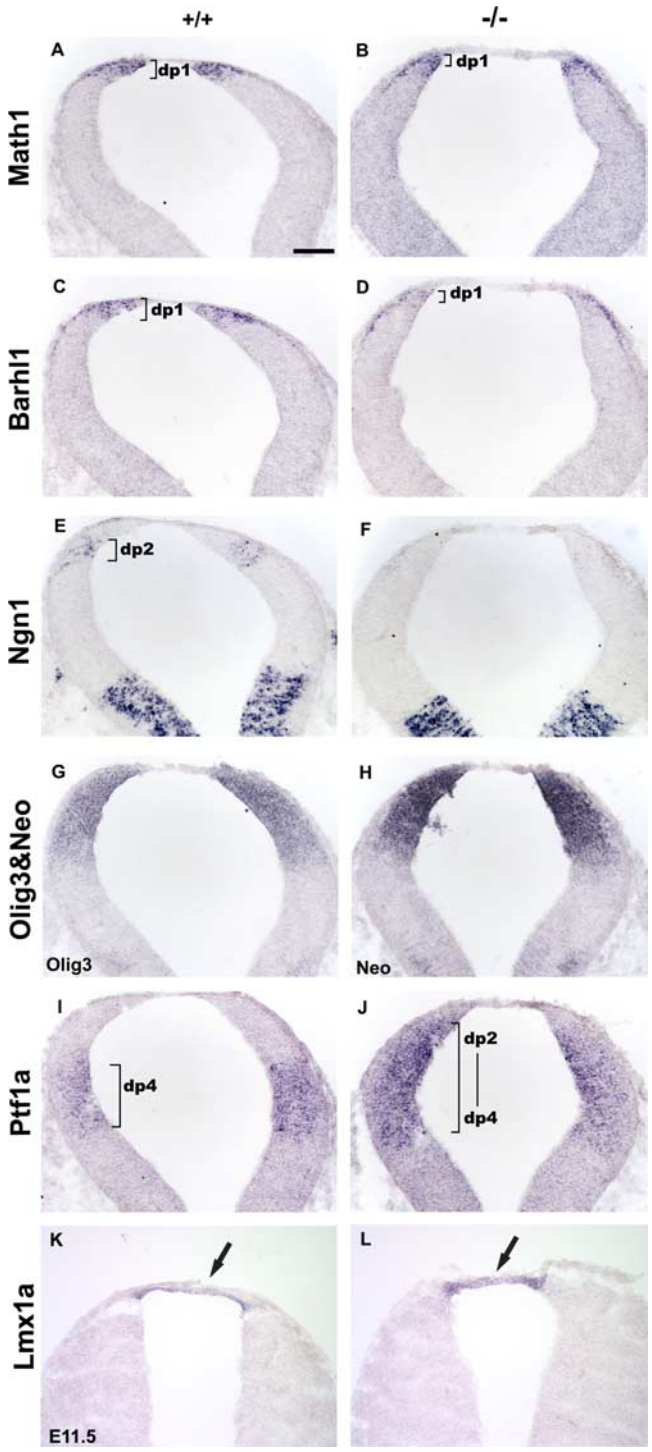

Figure 6. Altered gene expression in cRL of *Olig3*-null embryos. ***A–L***, Hindbrain sections from E10.5 embryos at the cRL level were subjected to *in situ* hybridization with riboprobes for *Math1* (***A***, ***B***), *Barhl1* (***C***, ***D***), *Ngn1* (***E***, ***F***), *Olig3* (***G***), *Neo* (***H***), *Ptf1a* (***I***, ***J***), and *Lmx1a* (***K***, ***L***). Loss of *Olig3* significantly downregulated the expression level of *Math1*, *Ngn1*, and *Barhl1*, whereas *Ptf1a* expression was ectopically expanded into dp2– dp3 domains. The expression pattern of *Neo* in *Olig3* mutant was the same as that of *Olig3* in wild-type controls (***G***, ***H***). ***K***, ***L***, Arrows indicate *Lmx1a* expression in the roof plate. Scale bar, 100 μm.

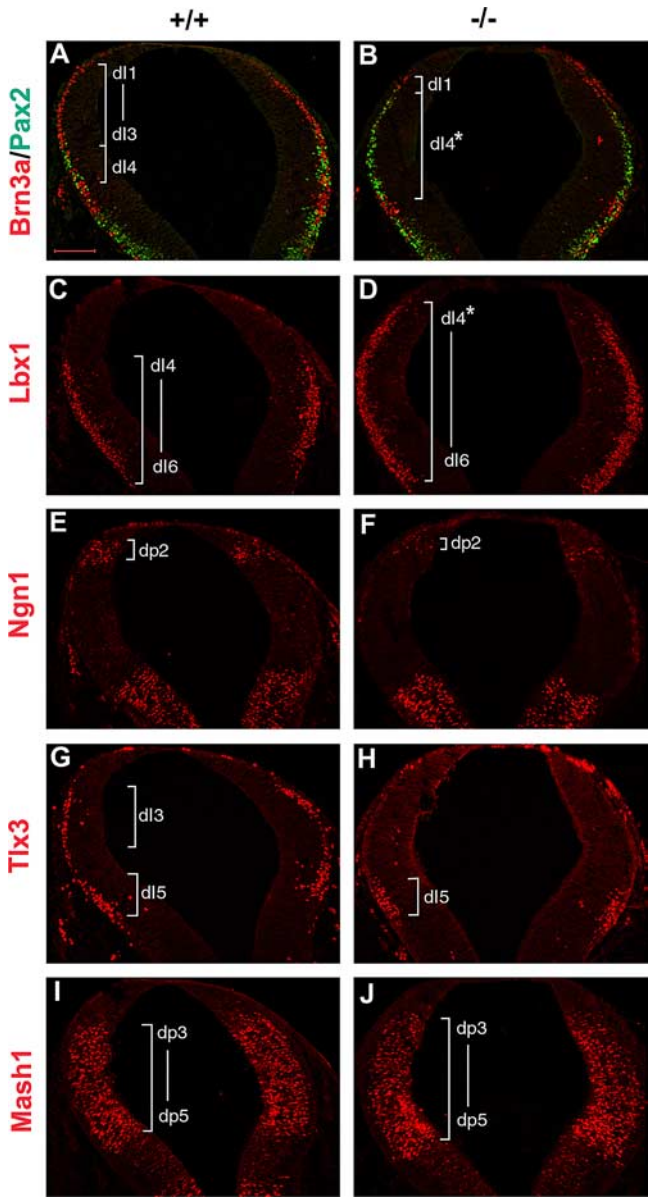

Figure 7. *Olig3* is important for the specification of cRL. ***A–J***, Coronal sections of E10.5 cRL were assessed by immunostaining with Brn3a and Pax2 (***A***, ***B***), Lbx1 (***C***, ***D***), Ngn1 (***E***, ***F***), Tlx3 (***G***, ***H***), and Mash1 (***I***, ***J***). The *Olig3*−/− mutant lost the expression of Brn3a in dI2– dI3 neurons and Tlx3 in dI3 neurons, and had a reduced number of Ngn1+ progenitor cells in dp2 domain. Ectopic expression of Pax2 and Lbx1 was detected at the positions of dI2– dI3 neurons. ***B***, ***D***, dI4* indicates ectopic dI4 interneurons derived from dp2 and dp3 domains in *Olig3*−/− hindbrain. Expression of Mash1 in the dp3– dp5 domains was not altered. Scale bar, 100 μm.

ithelium in the caudal hindbrain could completely inhibit the formation of ION comprised of CF neurons (Harkmark, 1954). Our results suggested that CF neurons are derived from the *Olig3*-expressing domains. In *Olig3* mutant embryos, dI2 and dI3 Brn3a+ neurons were not produced, in parallel to the complete loss of Brn3a+ CF neurons in the ION. Together, these findings suggested that cRL can be divided into two regions along dorsal–ventral axis: the dp1 progenitor domain that gives rise to the precerebellar MF neurons and the ventral *Olig3*+ progenitor domains that contribute substantially to the formation of precerebellar CF nucleus.

Recent Ptf1a-Cre lineage tracing experiments showed that Brn3a+ glutamatergic CF neurons are derived from *Ptf1a*+ progenitor cells, and *Ptf1a*-null mutation similarly resulted in the loss of ION (Hoshino et al., 2005; Yamada et al., 2007). In light of our finding that *Ptf1a* was coexpressed with *Olig3* in the ventral dp3 domain and a dual requirement of *Ptf1a* and *Olig3* for ION formation (Figs. 1*K*, 2*A*), we propose that CF neurons are spe-

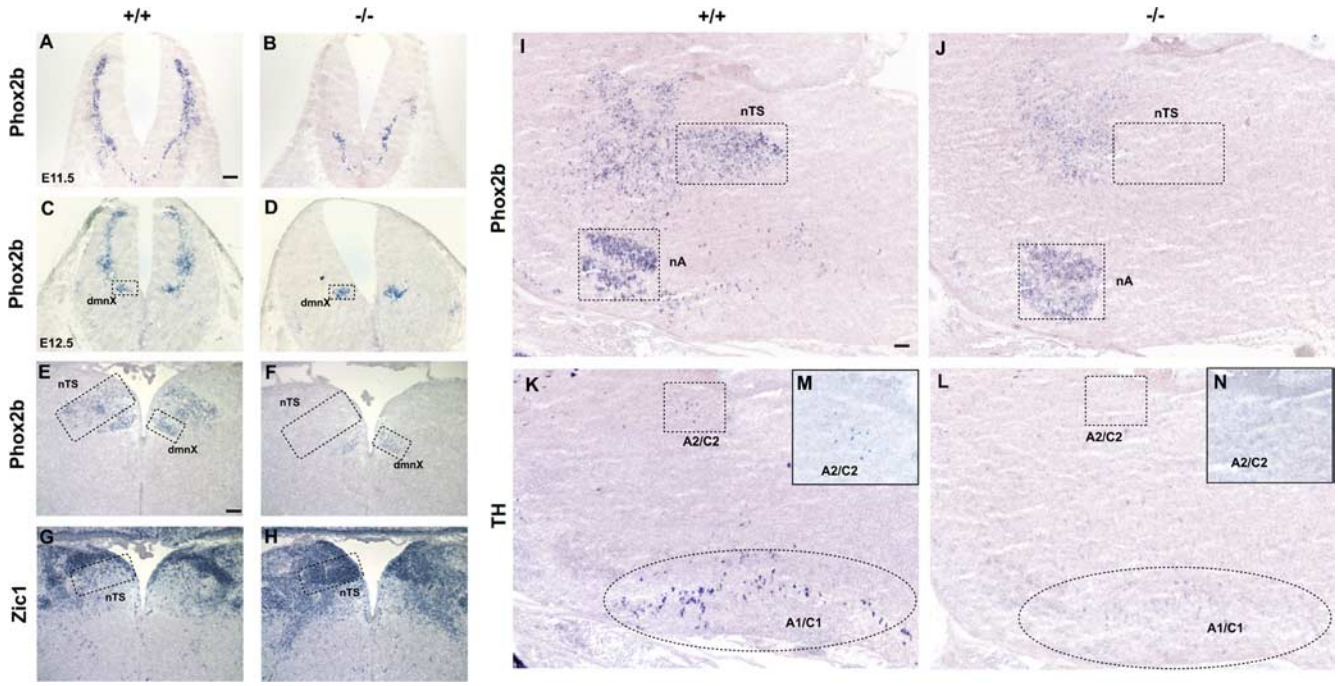

Figure 8. Formation of brainstem (nor)adrenergic centers and first-order relay visceral sensory neurons is dependent on *Olig3*. ***A–D***, *Phox2b* expression was examined in the transverse sections of E11.5 (***A***, ***B***) and E12.5 (***C***, ***D***) caudal hindbrains. Dorsal expression of Phox2b was completely inhibited in Olig3 mutants. ***E***, ***F***, The nTS labeled with *Phox2b* was lost in E18.5 *Olig3* mutants, whereas the dmnX, located ventral to the nTS structure in wild-type embryos (***E***), still existed in *Olig3*−/− medulla (***F***). ***G***, ***H***, Ectopic *Zic1* expression was detected in the prospective nTS area in *Olig3* mutants. ***I–L***, All E18.5 sagittal sections were oriented with rostral to the left. ***I***, ***J***, *Phox2b* expression was checked in the sagittal sections. ***K***, ***L***, In *Olig3* mutants, expression of *TH* was absent in the (nor)adrenergic centers of medulla, including A1/C1 and A2/C2. ***M***, ***N***, High-power images of A2/C2 areas. Scale bars: ***A*** (for ***A–D***), ***E*** (for ***E–H***), ***I*** (for ***I–L***), 100 μm.

cifically derived from the *Olig3*+/*Ptf1a*+ overlapping region of the ventral dp3 domain (Fig. 1*K*). Although *Olig3* is required for the fate specification of Brn3a+ excitatory CF neurons, *Ptf1a* activity appears to be essential for the proper migration of CF neurons. In the absence of *Ptf1a* expression, the generation of Brn3a+ neurons was not compromised, but these neurons failed to migrate into the ION area and subsequently underwent apoptosis (Yamada et al., 2007).

Ptf1a is also expressed in dp4 progenitor cells that give rise to inhibitory neurons (Fig. 1*C*,*F*,*J*,*K*). In *Olig3* mutant embryos, the *Ptf1a* expression was dorsally expanded in association with the dorsal expansion of Pax2+/Lbx1+ GABAergic neurons at the expense of Tlx3+/Brn3a+ glutamatergic neurons (Figs. 6*I*,*J*, 7*A–D*,*G*,*H*). As a result, the formation of Brn3a+ IMS of CF neurons and ION were completely abolished (Fig. 5; supplemental Figs. S1, S2, available at www.jneurosci.org as supplemental material). Collectively, these findings strongly suggested that in the absence of *Olig3* expression, the dp2 and dp3 domains were respecified to the dp4 domain. In contrast, the generation of Brn3a+/Tlx3+ dI5 neurons was not affected (Fig. 7*A*,*B*,*G*,*H*), indicating that dI5 neurons do not contribute to ION population.

ION is largely composed of glutamatergic excitatory neurons (Brn3a+), but it also contains a small number of GABAergic inhibitory neurons (Fredette et al., 1992). The inhibitory ION neurons may originate from the more ventral *Ptf1a* domain of dorsal caudal hindbrain. The *Ptf1a*+ neural progenitor cells in dp4 domain are in close association with the Pax2+ neurons, consistent with the previous reports that *Ptf1a* promotes the fate of GABAergic inhibitory neurons in the dorsal spinal cord and cerebellum (Glasgow et al., 2005; Hoshino et al., 2005).

Olig3 deficiency inhibits the development of the central respiratory center

Olig3−/− mutants died at birth and displayed cyanosis, suggesting that *Olig3* function is related to the development of the respiratory system. In support of this idea, *Olig3* regulates the specification of dI1–dI3 interneurons, which contribute substantially to the diversity of cell types within the respiratory system. *Olig3* mutation may affect several regulatory pathways that are important for the development of the respiratory system. First, loss of *Olig3* function significantly affected the formation of four precerebellar MF nuclei through *Math1* regulatory pathway (Fig. 4). In particular, the LRN is located in the ventrolateral region of the medulla, where the ventral medullary respiratory center resides. Development of LRN neurons might be particularly important for the functioning of respiratory system. Consistent with this idea, *Math1*-null mice died shortly after birth from respiratory failure (Ben-Arie et al., 1997). Second, absence of *Olig3* completely inhibited the generation of *Phox2b*+ neurons from dI3 domain and subsequently disrupted the formation of brainstem (nor)adrenergic centers and first-order relay visceral sensory neurons that were critical for respiratory rhythms and cardiovascular control (Fig. 8). It is well known that *Phox2b* is an important transcription factor regulating respiratory activity; mutations in *Phox2b* are the main disease-defining mutation in human congenital central hypoventilation syndrome (CCHS), leading to life-threatening hypoxia immediately after birth (Amiel et al., 2003). *Tlx3*-null mice lost the expression of *Phox2b* at later embryonic stages and showed a rapid respiratory rate with short inspiratory duration and frequent apnea (Shirasawa et al., 2000; Qian et al., 2001). Third, *Olig3* mutation resulted in the misspecification of dI2–dI3 neurons into dI4 interneurons, and *Ptf1a* was

ectopically expressed in dp2–dp3 domains (Fig. 6*I*,*J*). Tlx3 expression in dp3 domain was lost in *Olig3* mutant hindbrain (Fig. 7*G*,*H*). Previous reports demonstrated that *Ptf1a* promoted neural precursors to differentiate into GABAergic neurons and Tlx3 determined glutamatergic over GABAergic cell fates (Cheng et al., 2004, 2005; Glasgow et al., 2005; Hoshino et al., 2005; Mizuguchi et al., 2006). Consistent with these findings, ectopic expression of *Viaat*, a GABAergic neuron marker, was detected at the nTS area in E18.5 *Olig3*-deficient embryos (supplemental Fig. S3*G*,*H*, available at www.jneurosci.org as supplemental material). Thus, excess GABAergic neurons existed in *Olig3* mutant respiratory circuit, and this could alter the respiratory pattern, offering an alternative explanation for the change of respiratory rhythm in *Tlx3* mutant mice. Together, these observations strongly suggest that *Olig3* is an important transcription factor regulating the embryonic development of the central respiratory system. Human sudden infant death syndrome (SIDS) is a major cause of infant mortality, but the exact cause of this disease is still unclear. Growing evidence suggests that the impairment of central respiratory control leads to the defect of SIDS patients in response to breath and blood pressure challenges during sleep (Gillan et al., 1989). In addition, one-third of CCHS victims do not carry the mutation of *Phox2b* gene (Amiel et al., 2003). Therefore, *Olig3* should be a candidate gene for human SIDS and CCHS.

References

Altman J, Bayer SA (1987a) Development of the precerebellar nuclei in the rat: I. The precerebellar neuroepithelium of the rhombencephalon. J Comp Neurol 257:477–489.

Altman J, Bayer SA (1987b) Development of the precerebellar nuclei in the rat: II. The intramural olivary migratory stream and the neurogenetic organization of the inferior olive. J Comp Neurol 257:490–512.

Altman J, Bayer SA (1987c) Development of the precerebellar nuclei in the rat: III. The posterior precerebellar extramural migratory stream and the lateral reticular and external cuneate nuclei. J Comp Neurol 257:513–528.

Altman J, Bayer SA (1987d) Development of the precerebellar nuclei in the rat: IV. The anterior precerebellar extramural migratory stream and the nucleus reticularis tegmenti pontis and the basal pontine gray. J Comp Neurol 257:529–552.

Ambrosiani J, Armengol JA, Martinez S, Puelles L (1996) The avian inferior olive derives from the alar neuroepithelium of the rhombomeres 7 and 8: an analysis by using chick-quail chimeric embryos. Neuroreport 7:1285–1288.

Amiel J, Laudier B, Attié-Bitach T, Trang H, De Pontual L, Gener B, Trochet D, Etchevers H, Ray P, Simonneau M, Vekemans M, Munnich A, Gaultier C, Lyonnet S (2003) Polyalanine expansion and frameshift mutations of the paired-like homeobox gene Phox2B in congenital central hypoventilation syndrome. Nat Genet 33:459–461.

Belluardo N, Wu G, Mudo G, Hansson AC, Pettersson R, Fuxe K (1997) Comparative localization of fibroblast growth factor receptor-1, -2, and -3 mRNAs in the rat brain: in situ hybridization analysis. J Comp Neurol 379:226–246.

Ben-Arie N, Bellen HJ, Armstrong DL, McCall AE, Gordadze PR, Guo Q, Matzuk MM, Zoghbi HY (1997) Math1 is essential for genesis of cerebellar granule neurons. Nature 390:169–172.

Blessing W (1997) The lower brainstem and body homeostasis. New York: Oxford UP.

Bulfone A, Menguzzato E, Broccoli V, Marchitiello A, Gattuso C, Mariani M, Consalez GG, Martinez S, Ballabio A, Banfi S (2000) Barhl1, a gene belonging to a new subfamily of mammalian homeobox genes, is expressed in migrating neurons of the CNS. Hum Mol Genet 9:1443–1452.

Cambronero F, Puelles L (2000) Rostrocaudal nuclear relationship in the avian medulla oblongata: a fate map with quail chick chimeras. J Comp Neurol 427:522–545.

Caspary T, Anderson KV (2003) Patterning cell types in the dorsal spinal cord: what the mouse mutants say. Nat Rev Neurosci 4:289–297.

Cheng L, Arata A, Mizuguchi R, Qian Y, Karunaratne A, Gray PA, Arata S, Shirasawa S, Bouchard M, Luo P, Chen CL, Busslinger M, Goulding M, Onimaru H, Ma Q (2004) Tlx3 and Tlx1 are post-mitotic selector genes determining glutamatergic over GABAergic cell fates. Nat Neurosci 7:510–517.

Cheng L, Samad OA, Xu Y, Mizuguchi R, Luo P, Shirasawa S, Goulding M, Ma Q (2005) Lbx1 and Tlx3 are opposing switches in determining GABAergic versus glutamatergic transmitter phenotypes. Nat Neurosci 8:1510–1515.

Farago AF, Awatramani RB, Dymecki SM (2006) Assembly of the brainstem cochlear nuclear complex is revealed by intersectional and subtractive genetic fate maps. Neuron 50:205–218.

Fedtsova NG, Turner EE (1995) Brn-3.0 expression identifies early post-mitotic CNS neurons and sensory neural precursors. Mech Dev 53:291–304.

Fink AJ, Englund C, Daza RA, Pham D, Lau C, Nivison M, Kowalczyk T, Hevner RF (2006) Development of the deep cerebellar nuclei: transcription factors and cell migration from the rhombic lip. J Neurosci 26:3066–3076.

Foletti DL, Scheller RH (2001) Developmental regulation and specific brain distribution of phosphorabphilin. J Neurosci 21:5461–5472.

Fredette BJ, Adams JC, Mugnaini E (1992) GABAergic neurons in the mammalian inferior olive and ventral medulla detected by glutamate decarboxylase immunocytochemistry. J Comp Neurol 321:501–514.

Gillan JE, Curran C, O'Reilly E, Cahalane SF, Unwin AR (1989) Abnormal patterns of pulmonary neuroendocrine cells in victims of sudden infant death syndrome. Pediatrics 84:828–834.

Glasgow SM, Henke RM, MacDonald RJ, Wright CVE, Johnson JE (2005) Ptf1a determines GABAergic over glutamatergic neuronal cell fate in the spinal cord dorsal horn. Development 132:5461–5469.

Gowan K, Helms AW, Hunsaker TL, Collisson T, Ebert PJ, Odom R, Johnson JE (2001) Crossinhibitory activities of Ngn1 and Math1 allow specification of distinct dorsal interneurons. Neuron 31:219–232.

Gross MK, Dottori M, Goulding M (2002) Lbx1 specifies somatosensory association interneurons in the dorsal spinal cord. Neuron 34:535–549.

Harkmark W (1954) Cell migrations from the rhombic lip to the inferior olive, the nucleus raphe and the pons. A morphological and experimental investigation of chick embryos. J Comp Neurol 100:115–209.

Helms AW, Johnson JE (2003) Specification of dorsal spinal cord interneurons. Curr Opin Neurobiol 13:42–49.

His W (1891) Die Entwicklung des menschlichen rautenhirms vom ende des ersten bis zum beginn des dritten monats. I. Verlangertes mark. Abhandlungen der koniglicher sachsischen gesellschaft der wissenschaften. Mathematische-physikalische Klasse 29:1–74.

Hoshino M, Nakamura S, Mori K, Kawauchi T, Terao M, Nishimura YV, Fukuda A, Fuse T, Matsuo N, Sone M, Watanabe M, Bito H, Terashima T, Wright CV, Kawaguchi Y, Nakao K, Nabeshima Y (2005) Ptf1a, a bHLH transcriptional gene, defines GABAergic neuronal fates in cerebellum. Neuron 47:201–213.

Jessell TM (2000) Neuronal specification in the spinal cord: inductive signals and transcriptional codes. Nat Rev Genet 1:20–29.

Landsberg RL, Awatramani RB, Hunter NL, Farago AF, DiPietrantonio HJ, Rodriguez CI, Dymecki SM (2005) Hindbrain rhombic lip is comprised of discrete progenitor cell populations allocated by Pax6. Neuron 48:933–947.

Lee KJ, Jessell TM (1999) The specification of dorsal cell fates in the vertebrate central nervous system. Annu Rev Neurosci 22:261–294.

Lumsden A, Krumlauf R (1996) Patterning the vertebrate neuraxis. Science 274:1109–1115.

Machold R, Fishell G (2005) Math1 is expressed in temporally discrete pools of cerebellar rhombic-lip neural progenitors. Neuron 48:17–24.

Mizuguchi R, Kriks S, Cordes R, Gossler A, Ma Q, Goulding M (2006) Ascl1 and Gsh1/2 control inhibitory and excitatory cell fate in spinal sensory interneurons. Nat Neurosci 9:770–778.

Morin X, Cremer H, Hirsch MR, Kapur RP, Goridis C, Brunet JF (1997) Defects in sensory and autonomic ganglia and absence of locus coeruleus in mice deficient for the homeobox gene Phox2a. Neuron 18:411–423.

Müller T, Brohmann H, Pierani A, Heppenstall PA, Lewin GR, Jessell TM, Birchmeier C (2002) The homeodomain factor lbx1 distinguishes two major programs of neuronal differentiation in the dorsal spinal cord. Neuron 34:551–562.

Müller T, Anlag K, Wildner H, Britsch S, Treier M, Birchmeier C (2005) The bHLH factor Olig3 coordinates the specification of dorsal neurons in the spinal cord. Genes Dev 19:733–743.

Pattyn A, Morin X, Cremer H, Goridis C, Brunet JF (1999) The homeobox gene Phox2b is essential for the development of autonomic neural crest derivates. Nature 399:366–370.

Pattyn A, Goridis C, Brunet JF (2000) Specification of the central noradrenergic phenotype by the homeobox gene Phox2b. Mol Cell Neurosci 15:235–243.

Qian Y, Fritzsch B, Shirasawa S, Chen CL, Choi Y, Ma Q (2001) Formation of brainstem (nor)adrenergic centers and first-order relay visceral sensory neurons is dependent on homeodomain protein Rnx/Tlx3. Genes Dev 15:2533–2545.

Qian Y, Shirasawa S, Chen CL, Cheng L, Ma Q (2002) Proper development of relay somatic sensor neurons and D2/D4 interneurons requires homeobox genes Rnx/Tlx3 and Tlx1. Genes Dev 16:1220–1233.

Schaeren-Wiemers N, Gerfin-Moser A (1993) A single protocol to detect transcripts of various types and expression levels in neural tissue and cultured cells: in situ hybridization using digoxigenin-labeled cRNA probes. Histochemistry 100:431–440.

Schüller U, Kho AT, Zhao Q, Ma Q, Rowitch DH (2006) Cerebellar 'transcriptome' reveals cell-type and stage-specific expression during postnatal development and tumorigenesis. Mol Cell Neurosci 33:247–259.

Shirasawa S, Arata A, Onimaru H, Roth KA, Brown GA, Horning S, Arata S, Okumura K, Sasazuki T, Korsmeyer SJ (2000) Rnx deficiency results in congenital central hypoventilation. Nat Genet 24:287–290.

Sieber MA, Storm R, Martinez-de-la-Torre M, Müller T, Wende H, Reuter K, Vasyutina E, Birchmeier C (2007) Lbx1 acts as a selector gene in the fate determination of somatosensory and viscerosensory relay neurons in the hindbrain. J Neurosci 27:4902–4909.

Sotelo C (2004) Cellular and genetic regulation of the development of the cerebellar system. Prog Neurobiol 72:295–339.

Takebayashi H, Ohtsuki T, Uchida T, Kawamoto S, Okubo K, Ikenaka K, Takeichi M, Chisaka O, Nabeshima Y (2002) Non-overlapping expression of Olig3 and Olig2 in the embryonic neural tube. Mech Dev 113:169–174.

Wang VY, Rose MF, Zoghbi HY (2005) Math1 expression redefines the rhombic lip derivatives and reveals novel lineages within the brainstem and cerebellum. Neuron 48:31–43.

Xiang M, Gan L, Zhou L, Klein WH, Nathans J (1996) Targeted deletion of the mouse POU domain gene Brn-3a causes selective loss of neurons in the brainstem and trigeminal ganglion, uncoordinated limb movement, and impaired suckling. Proc Natl Acad Sci U S A 93:11950–11955.

Yamada M, Terao M, Terashima T, Fujiyama T, Kawaguchi Y, Nabeshima Y, Hoshino M (2007) Origin of climbing fiber neurons and their developmental dependence on Ptf1a. J Neurosci 27:10924–10934.